

# PEM fuel cell stacks operated under dry-reactant conditions

Zhigang Qi\*, Arthur Kaufman

*H Power Corporation, 60 Montgomery Street, Belleville, NJ 07109, USA*

Received 21 February 2002; accepted 4 March 2002

## Abstract

A double-path-type flow-field design that has two gas inlets and two gas outlets is presented for PEM fuel cells. The two paths are arranged in such a way that the inlet of one flow-field is adjacent to the outlet of the other flow-field and, within any section of the electrode active area, there are always adjacent channels with reactant flowing in opposite directions. Such a design enables the dry entering gas to become hydrated by acquiring some moisture from the exiting moist gas; and, within any section of the active area, the drier gas in one flow-field can share the moisture in the wetter gas flowing in the other flow-field. Such a design effectively uses the water produced by the stack to hydrate the membrane and the catalyst layers. The effectiveness of this design was demonstrated by running multiple-cell stacks where the stack could run stably at a current density up to 0.33 A/cm<sup>2</sup> using dry hydrogen and dry air. © 2002 Elsevier Science B.V. All rights reserved.

*Keywords:* Double-path-type flow-field; PEM fuel cells; Stack

## 1. Introduction

Water plays a critical role in proton exchange membrane (PEM) fuel cells. Both the Nafion membrane and the Nafion material within the catalyst layers need to be hydrated in order to efficiently conduct protons. The proton conductivity increases with the water content [1–3]. The water content can be expressed by a weight percentage, or more often by the number of water molecules held by each sulphonate group. In order to achieve enough hydration, water is normally introduced into the cell externally by a variety of methods such as liquid injection, steam introduction, and humidification of reactants by passing them through humidifiers before entering the cell. Humidification by the last method is relatively easier to handle, and therefore, it is the most commonly used method. In order to simplify the system and to limit the amount of water to carry for the humidification purpose, the water generated by the fuel cell at the cathode should be utilized as much as possible. The water in the exhaust air can be captured by the membrane in a membrane-type humidifier or by molecular sieve material in rotating apparatus, and then transported to the reactants as they separately pass through the apparatus. Membrane-type humidifiers can also be incorporated as part of the electrolyte

membrane of a cell, or can be constructed as part of a fuel cell stack [4,5].

H Power Corporation has been using the water generated by the fuel cell to humidify the dry reactants through the design of double-path-type flow-fields or other configurations with counter-current reactant flow characteristics [6]. Typically, a single-path flow-field is used by various fuel cell developers. In such a flow-field the reactant enters the cell from one location, flows through the channels, and finally exits from another location. If no external humidification is used, such a flow-field will cause uneven humidification along the gas flow path. Near the entrance, the cell will be very dry, because the gas is dry. As the gas proceeds along the flow path, water content increases because the gas can accumulate more water that is produced by the fuel cell. Hence, near the exit the hydration level will be the highest. The disparity might get even worse as time progresses. The dry area will creep deeper into the flow-field, causing more area to work inefficiently. In order to avoid such uneven humidification, H Power has invented a double-path-type flow-field design as shown in Fig. 1, as well as related designs to accomplish the same objective. In this design, two flow-fields, serpentine, straight, or any other shapes, are placed side-by-side. One flow-field's inlet is located near the other's outlet and, within any section of the electrode active area, there are always adjacent channels with reactant flowing in opposite directions (solid and empty arrows were used to show the flow of reactant in the two flow-fields, respectively). Such a design enables the dry entering gas to

\* Corresponding author. Tel.: +1-973-450-4400x478;  
fax: +1-973-450-9850.  
E-mail address: zqi@hpower.com (Z. Qi).

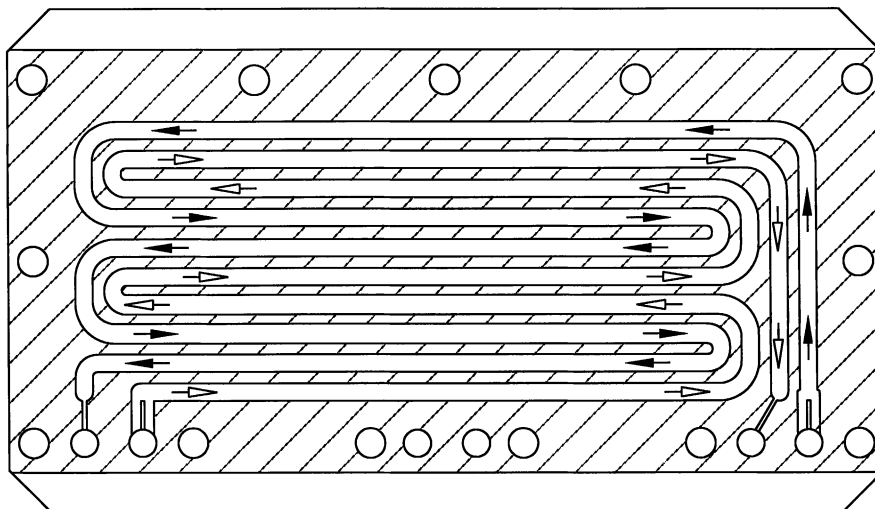


Fig. 1. A double-path-type flow-field design.

become hydrated by acquiring some of the moisture from the exiting wet gas; and, within any section of the active area, the drier gas in one flow-field can share the moisture in the wetter gas flowing in the other flow-field. Therefore, the uneven humidification experienced by the single-path flow-field design is avoided; and the entire cell achieves a more even humidification.

Another advantage of double-path-type flow-fields is that it can also achieve a more even reactant concentration distribution over the entire electrode active area. In a single-path flow-field, the reactant has the highest and lowest concentration at the entrance and exit, respectively, because, as the reactant-flow proceeds, it is consumed by the electrochemical reaction. Such an uneven concentration distribution causes an uneven current distribution. What is worse is that some “hot spots” may be created at places with very low reactant concentration. Such hot spots may accelerate membrane deterioration. With double-path-type flow-fields, the reactant will distribute more evenly and thereby avoid these problems.

The effectiveness of double-path-type flow-fields has been tested in multiple-cell stacks with various active areas. This article presents data obtained by using four-cell stacks with an active area of  $27.6 \text{ cm}^2$  per cell.

## 2. Experimental

Electrodes with various catalyst, Nafion, and PTFE loadings were prepared and tested. For high Pt-loading electrodes ( $>1.0 \text{ mg/cm}^2$ ), Pt black was used as the catalyst. For electrodes with lower Pt loadings, 20% Pt/Vulcan XC-72 was used. The electrodes were prepared on teflonized carbon-paper-type gas diffusion media. These electrodes were hot-pressed onto Nafion membranes at  $130 \text{ }^\circ\text{C}$  for 3 min.

Fig. 2 shows the stack-assembly sequence for a two-cell stack. Tie rods were first fixed onto the cathode end plate. The plate could be made of metals or plastics with high mechanical strength so that it would not deform under a compressive load. An insulating gasket was then laid on, followed by a current collector, a gasket for the current collector, and the cathode termination plate. The insulating gasket is used to prevent electrical contact between the metal current collector and the end plate. The cathode termination plate has a flow-field only on one side, and the dotted line indicates that the flow-field is facing up. Above the termination plate there is a gasket for the cathode, a membrane-electrode assembly (MEA), a gasket for the anode, and a bipolar plate. The bipolar plate has flow-fields on both sides with the bottom side for anode and the top side for cathode. In this case the anode flow-field is illustrated as a serpentine single-path, and the cathode flow-field with serpentine double-paths. The stacking steps repeat until the anode end plate is placed. The stack is then tightened by screws at a suitable torque.

The stacks were operated with dead-ended hydrogen; i.e. the hydrogen exit was closed. Such a configuration should achieve fuel utilization close to 100%. Periodically, purging was performed to release liquid water and any impurities that accumulated during operation by opening the hydrogen exit for a very short period (fraction of a second). The opening and closing of the exit valve were controlled by a solenoid. The air exit was open to the atmosphere, and its flow was controlled at a stoichiometry of three times using a metering valve and a flow meter. The inlet pressure of the hydrogen was set at ca. 5 psig. Unless specified, neither hydrogen nor air was humidified. We refer to unhumidified reactants as dry reactants throughout this paper, although air has its natural humidity. The stack temperature was controlled by two small fans placed adjacent to the stack. The voltage–current density curves were collected using an HP 6050 A load bank.

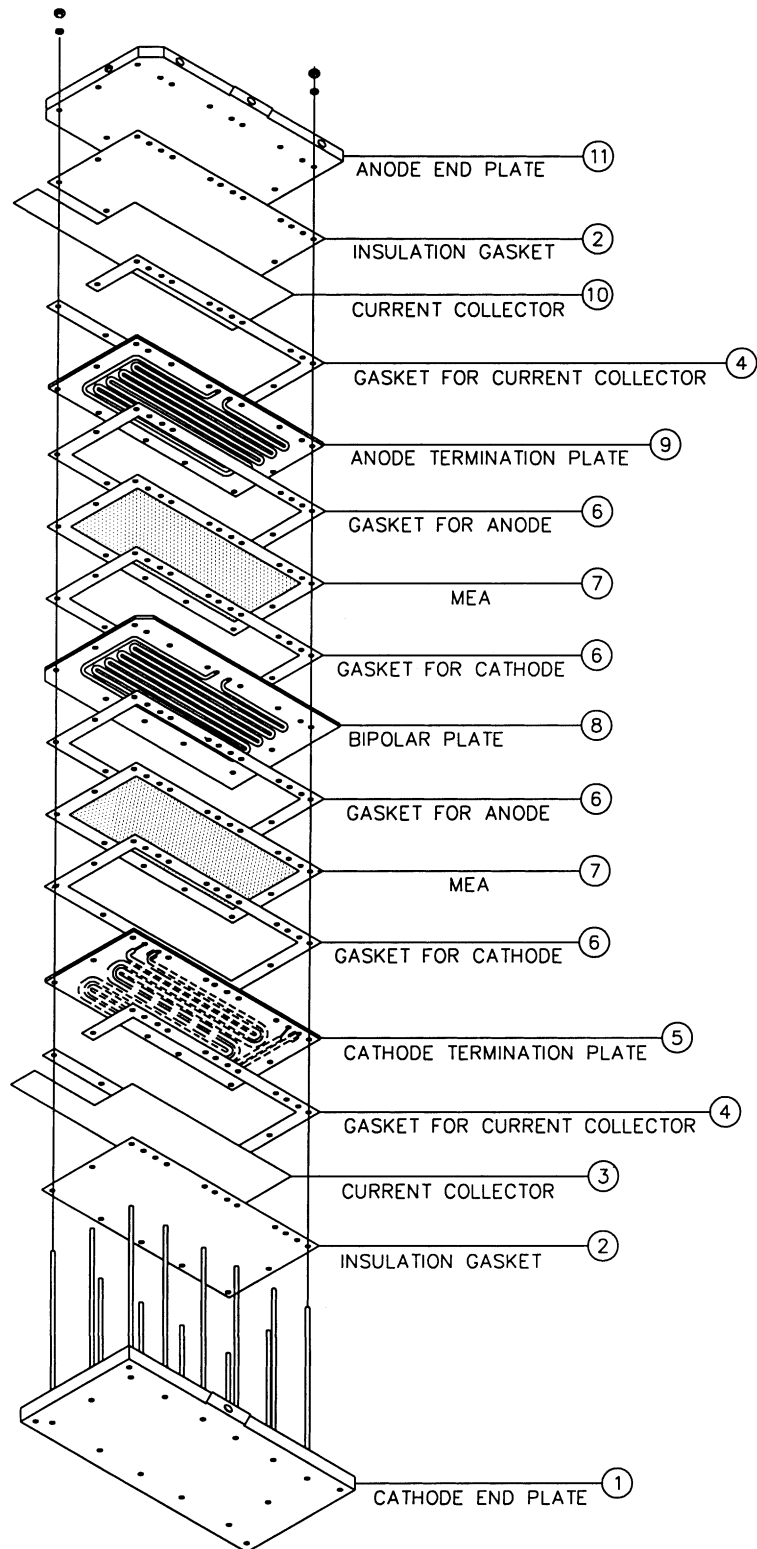


Fig. 2. A stack-assembly sequence.

### 3. Results and discussion

Fig. 3 shows how voltage changes with current for a four-cell stack whose MEAs had a Pt loading of 1.7 mg/cm<sup>2</sup> for

both anode and cathode. As the current was set sequentially to 4, 6, 7, and 8 A during the first 5 h, the corresponding stack voltage (average) was 2.8, 2.5, 2.3, and 2.0 V, respectively. The stack was then operated at a current of 6 A for

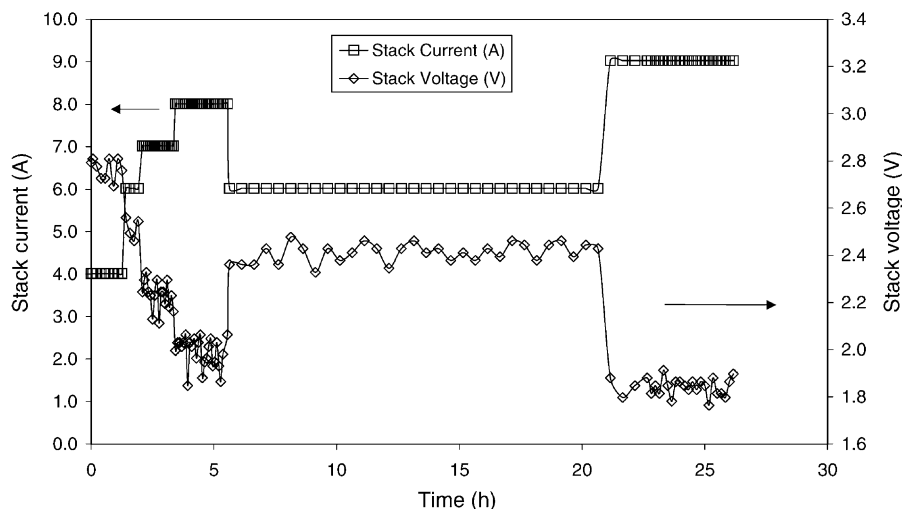


Fig. 3. Current and voltage for a four-cell stack using electrodes with Pt loading of  $1.7 \text{ mg/cm}^2$ , Nafion 112 membrane.

>15 h. The stack voltage oscillated slightly around 2.4 V without showing any sign of declining. The current was finally raised to 9 A for >5 h. During this period, the stack gave a stable voltage output of 1.80 V. A current of 9 A corresponds to a current density of  $0.33 \text{ A/cm}^2$  ( $27.6 \text{ cm}^2$  active area). It is quite unusual for a stack to run stably at such a current density without any external humidification.

A similar four-cell stack was tested using MEAs whose anode Pt loading was  $0.20 \text{ mg/cm}^2$ , while the cathode Pt loading was still  $1.7 \text{ mg/cm}^2$  (Fig. 4). This stack was operated continuously for nearly 80 h while the current was varied between 4 and 9 A. During the 60 h of operation at 6 A, the stack voltage declined from 2.45 to 2.30 V in the first 2 h, then it stabilized at 2.3 V. This voltage was only 0.1 V less than that of the previous stack, indicating that the anode Pt loading has little effect on the stack performance.

It has been found that performance is generally retained at these levels when the cathode loading (using supported catalysts) is reduced to the  $0.4\text{--}0.5 \text{ mg Pt/cm}^2$  level. However, the situation changed when the cathode Pt loading was decreased to about  $0.2 \text{ mg Pt/cm}^2$ . Fig. 5 shows the performance of a stack using MEAs with both anode and cathode Pt loadings of  $0.21 \text{ mg/cm}^2$ . The stack current was increased gradually from 0.5 to 2.5 A in the first 20 min to slowly boost the stack's ability to maintain a higher current. If the stack was directly applied a current of 2.5 A in the very beginning, its voltage declined quickly to nearly 0 V. This was the biggest difference from the higher Pt-loading cathode stacks, which could sustain higher currents immediately. When a current of 4 A was applied, the stack had a voltage of 1.65 V in the first 60 min, and increased to 2.4 V 30 min later. This voltage was quite stable during the following 140 h operation at 4 A. Fig. 6 shows only the results after

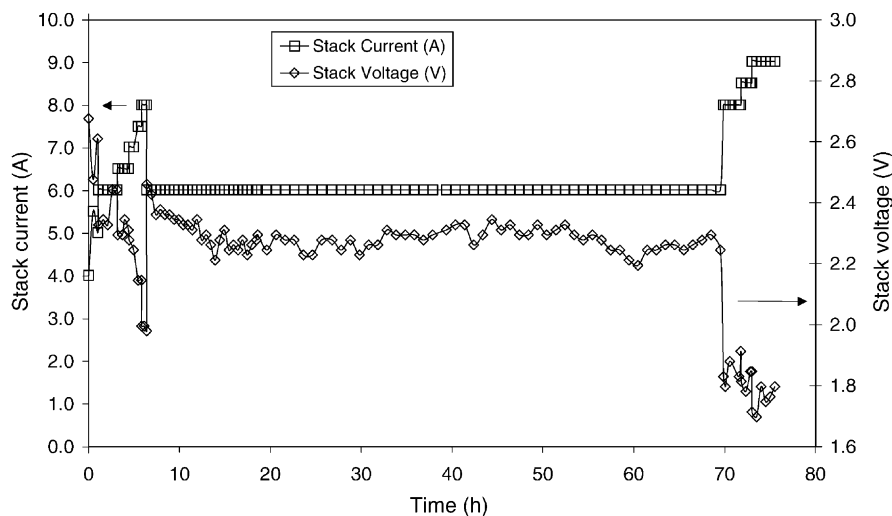


Fig. 4. Current and voltage for a four-cell stack using anode with Pt loading of  $0.20 \text{ mg/cm}^2$  and cathode with Pt loading of  $1.7 \text{ mg/cm}^2$ , Nafion 112 membrane.

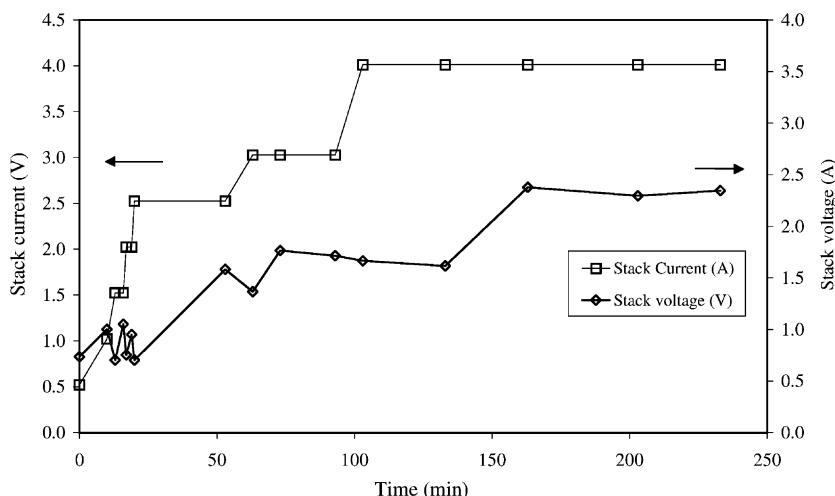


Fig. 5. Current and voltage for a four-cell stack in the first 4 h using electrodes with Pt loading of 0.21 mg/cm<sup>2</sup>, Nafion 1135 membrane.

136 h. Such a voltage was about 0.4 V lower than that of the previous stacks with higher Pt-loadings. When the current was increased to 6 A, the stack voltage declined quickly in the beginning, and finally stabilized at 1.7 V. This voltage was about 0.6–0.7 V lower than that of the previous higher Pt-loading stacks. When the current was decreased to 4 A, the stack only recovered to a voltage of 2.2 V, which was about 0.2 V lower than the value before the stack was operated at 6 A. When some liquid water was injected into the cathode side, the stack voltage increased to the previous level. Obviously, running the stack at 6 A gradually dried the stack. Since the stack produced more water at a higher current, the drying was unlikely to have occurred at the cathode. It is more likely to have occurred at the anode, as more water was taken away by protons to the cathode side via electro-osmotic drag. The only water present in the anode comes from the back-diffusion of water through the membrane from the cathode side. Another factor that contributed to the lower performance of this stack was that Nafion 1135, rather than 112, was used as the membrane. A

thicker membrane not only has a higher ionic resistance, but also is more difficult to hydrate. In addition, a thicker membrane reduces the amount of water that can back-diffuse from the cathode to the anode. This results in an even drier anode which can provide less water for the electro-osmotic drag by protons [7–9].

At an air stoichiometry of 2.5 times, all the previous stacks could run stably at a current of 4 A. Since no external humidification was used, it might be misleading to think that drying rather than flooding was the only issue. Actually, if the electrode can not manage water adequately, flooding or mass transport resistance due to flooding is also a problem. Fig. 7 shows the effect of air stoichiometry on the performance of a stack whose gas diffusion media were easily flooded. At 2.5 times air stoichiometry, the voltage decreased from 2.7 V to as low as 2.2 V in 70 min. When the air stoichiometry was increased to 3.3 times, the stack voltage increased to 2.7 V immediately. But with time, the voltage still declined. When the stoichiometry was further increased to 4.2 times, the stack voltage increased to 2.7 V

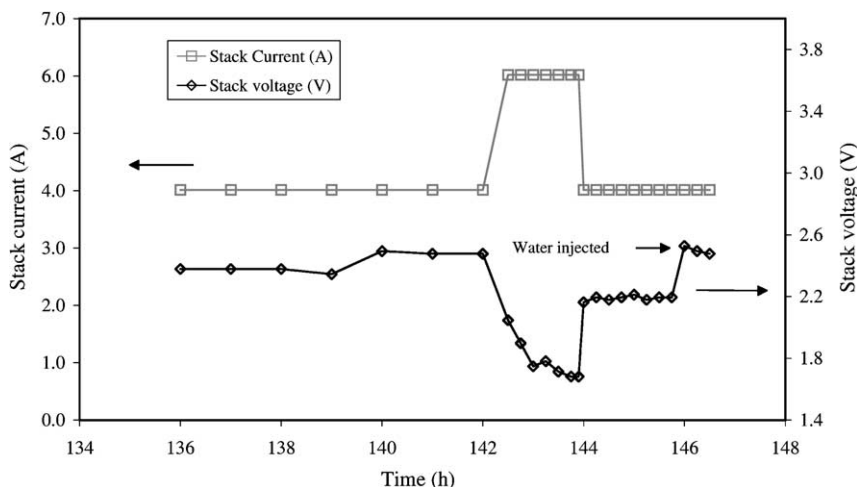


Fig. 6. Current and voltage for a four-cell stack in the last 10 h using electrodes with Pt loading of 0.21 mg/cm<sup>2</sup>, Nafion 1135 membrane.

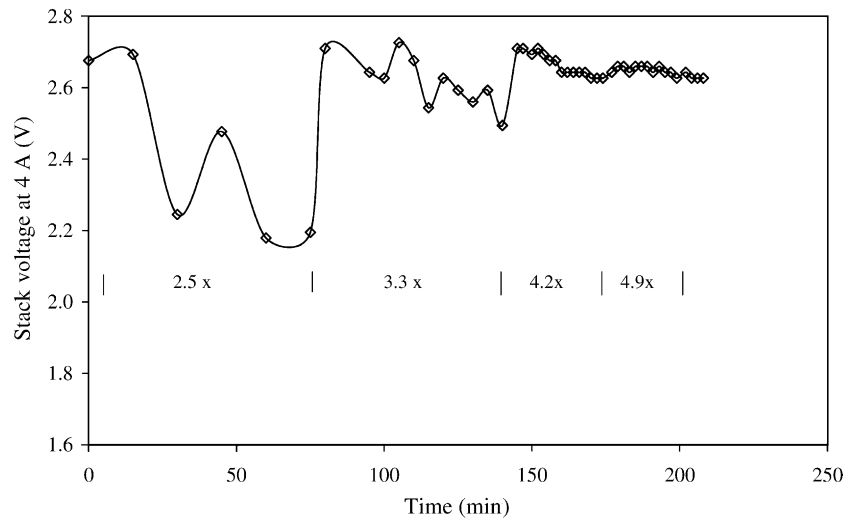


Fig. 7. Voltage change with air stoichiometry for a four-cell stack whose gas diffusion media were prone to flooding. Pt loading =  $1.7 \text{ mg/cm}^2$ , Nafion 1135 membrane.

again before sliding to 2.6 V. Increasing air stoichiometry to 4.9 times did not result in a further increase in stack voltage. At such a high stoichiometry, flooding was prevented, but the stack would be dried quickly.

Since there was no internal liquid cooling, the stack temperature was controlled by small fans. In a complete fuel cell system, the fans will be turned on automatically when the stack temperature goes above a pre-determined value. The stack temperature was measured by using a thermocouple that was inserted between the fins of the #2 and #3 cells for a four-cell stack. This temperature would be a little lower than the stack temperature in the center of each cell. The stack temperature is determined by the current density. Fig. 8 shows how the stack temperature increases with current density. At a current density  $<0.05 \text{ A/cm}^2$ , the stack temperature stayed at  $30^\circ\text{C}$ . However, when the current density was increased from 0.05 to  $0.40 \text{ A/cm}^2$ ,

the stack temperature increased from  $30$  to  $52^\circ\text{C}$  almost linearly. At temperatures  $>50^\circ\text{C}$ , the stack could be dried, so, it would be most suitable for operating in the low current density/high cell efficiency region.

Fig. 9 compares the performance of a stack using either dry or slightly humidified hydrogen. Hydrogen was humidified by passing it through a water bottle at room temperature. The purpose of choosing such a low humidification temperature was to prevent the accumulation of water in the anode compartment. Since the anode was designed to be dead-ended in order to achieve a 100% fuel usage, if the hydrogen was highly humidified, water could quickly accumulate to cause a decline in cell performance. The results of Fig. 9 indicated that lightly humidifying hydrogen could only slightly increase the stack performance.

Humidifying air could have a larger effect on performance as shown by Fig. 10. The Pt loading of both anode and

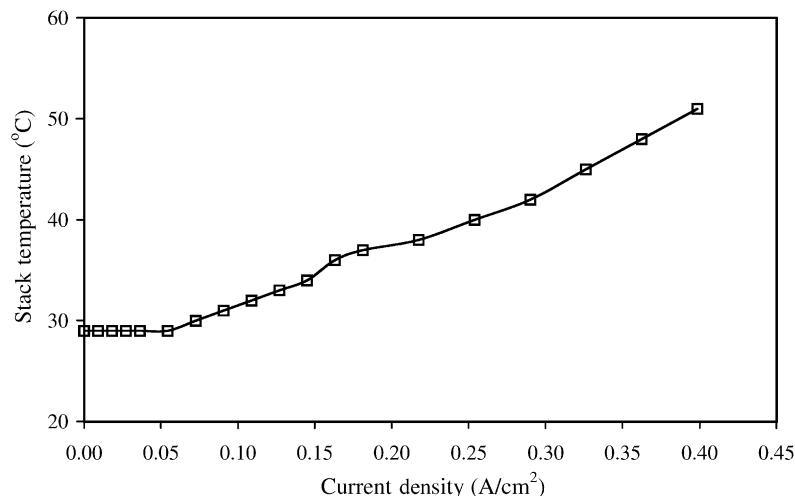


Fig. 8. Stack temperature vs. current density for a four-cell stack using electrodes with Pt loading of  $1.7 \text{ mg/cm}^2$ , Nafion 1135 membrane.

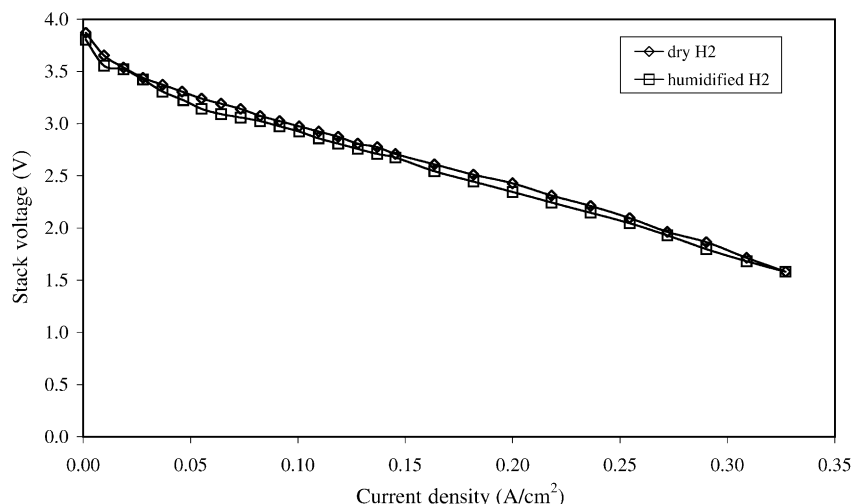


Fig. 9.  $V$ - $I$  curves of a four-cell stack using either dry or slightly humidified hydrogen. Pt loading =  $1.7 \text{ mg/cm}^2$ , Nafion 1135 membrane.

cathode for each of the four cells was  $1.7 \text{ mg/cm}^2$ , but different gas diffusion medium was used for each cell. The gas diffusion media were 10 mil Toray paper, 8.5, 10, and 12 mil experimental paper that all contained ca. 19% Teflon. These cells were assembled together into a four-cell stack so that the behavior of each gas diffusion medium could be compared side-by-side. Without air humidification, the cell voltages were 0.75, 0.61, 0.38 and 0.73 V at a current density of  $150 \text{ mA/cm}^2$  for the 10 mil Toray, 12, 10, and 8.5 mil experimental paper, respectively. The 10 mil experimental paper obviously gave an extremely low performance. When air was humidified at  $45^\circ\text{C}$ , the performance of the cells increased to 0.76, 0.67, 0.65, and 0.74 V, respectively. For the 10 mil Toray and 8.5 mil experimental substrates, humidifying air resulted in only very slight increase in performance. But for the 12 mil and especially the 10 mil experimental substrates, much larger increases were observed. This experiment indicates that the quality of

the gas diffusion media affects the water balance. The best would be those that do not lose water easily and at the same time are not flooded under the stack operation conditions. It is generally difficult to predict the behavior of a gas diffusion medium. The best way to know it has to be through testing.

The purpose of using unhumidified reactants is for simplicity. Such simplicity would be a necessity for using fuel cells as a portable power sources for mobile electronics. Although a double-path-type flow-field design enables a fuel cell to run at current densities up to  $0.33 \text{ A/cm}^2$  without drying out, the performance of the cell does suffer from insufficient water supply. The only water that is used to hydrate the membrane and the catalyst layers, and is used for electro-osmotic drag by protons comes from the reaction at the cathode. Even we ignore the amount of water taken out by exhaust air, and assume that all the water produced at cathode diffuses to the anode side, each proton would have a maximum of 0.5 water molecules to drag. This number is

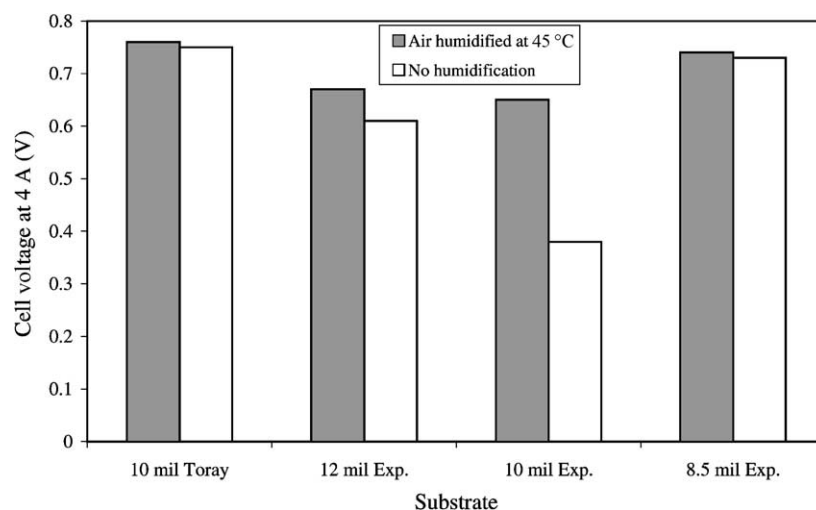


Fig. 10. Effect of air humidification on the performance of MEAs made using different substrates. Pt loading =  $1.7 \text{ mg/cm}^2$ , Nafion 1135 membrane.

much smaller than the number of water molecules (ca. 3) a proton can drag under fully hydrated conditions [10]. The insufficient amount of water molecules at the anode side for proton to drag would then seriously limit the performance of the cell.

Humidifying hydrogen would be most effective to change this situation. However, due to the use of a dead-ended hydrogen configuration in order to achieve a 100% hydrogen usage, humidifying hydrogen could cause water accumulation in the anode compartment, which in turn would lower the performance. Humidifying air would result in more water diffusing to the anode side, and thus, to provide more water for protons to drag. Its effectiveness has been illustrated by the data shown in Fig. 10. However, humidifying either hydrogen or air will make the system more complicated and deviates from the initial intention for simplicity.

#### 4. Conclusions

A double-path-type counter-current flow-field design was presented and its effectiveness was demonstrated. Such a design not only better utilizes the water produced by the fuel cell to hydrate dry reactants, but also achieves a more even

distribution of reactants over the entire active area. A stack can run stably at a current density up to  $0.33 \text{ A/cm}^2$  using dry hydrogen and dry air. Such an achievement can pave the way for a near-term adoption of fuel cells as a power source for portable electronic systems.

#### References

- [1] G. Pourcelly, A. Oikonomou, C. Gavach, *J. Electroanal. Chem.* 287 (1990) 43–59.
- [2] M. Watanabe, Y. Satoh, C. Shimura, *J. Electrochem. Soc.* 140 (1993) 3190–3193.
- [3] T.E. Springer, M.S. Wilson, S. Gottesfeld, *J. Electrochem. Soc.* 140 (1993) 3513–3526.
- [4] N.E. Vanderborgh, J.C. Hedstrom, US Patent No. 4,973,530 (1990).
- [5] C.Y. Chow, B.M. Wozniczka, US Patent No. 5,382,478 (1995).
- [6] A. Kaufman, P.L. Terry, US Patent No. 5,776,625 (1998).
- [7] T.A. Zawodzinski, M. Neeman, L.O. Sillerud, S. Gottesfeld, *J. Phys. Chem.* 95 (1991) 6040–6044.
- [8] X. Ren, W. Henderson, S. Gottesfeld, *J. Electrochem. Soc.* 144 (1997) L267–L270.
- [9] S.J. Paddison, R. Paul, T.A. Zawodzinski, *J. Electrochem. Soc.* 147 (2000) 617–626.
- [10] T.A. Zawodzinski, C. Derouin, S. Radzinski, R.J. Sherman, V.T. Smith, T.E. Springer, S. Gottesfeld, *J. Electrochem. Soc.* 140 (1993) 1041–1047.